Available online at www.sciencedirect.com
ScienceDirect
Journal of Power Sources 158 (2006) 1317–1323
JOURNAL OF POWER SOURCES
www.elsevier.com/locate/jpowsour

Short communication

Performance of diagonal control structures at different operating conditions for polymer electrolyte membrane fuel cells

Maria Serra*, Attila Husar, Diego Feroldi, Jordi Riera

Institut de Robòtica i Informàtica Industrial, Universitat Politècnica de Catalunya, Consejo Superior de Investigaciones Científicas, C. Llorens i Artigas 4, 08028 Barcelona, Spain

Received 5 August 2005; received in revised form 29 September 2005; accepted 26 October 2005
Available online 10 January 2006

Abstract

This work is focused on the selection of operating conditions in polymer electrolyte membrane fuel cells. It analyses efficiency and controllability aspects, which change from one operating point to another. Specifically, several operating points that deliver the same amount of net power are compared, and the comparison is done at different net power levels. The study is based on a complex non-linear model, which has been linearised at the selected operating points. Different linear analysis tools are applied to the linear models and results show important controllability differences between operating points. The performance of diagonal control structures with PI controllers at different operating points is also studied. A method for the tuning of the controllers is proposed and applied. The behaviour of the controlled system is simulated with the non-linear model. Conclusions indicate a possible trade-off between controllability and optimisation of hydrogen consumption.

Keywords: PEMFC; Diagonal control; PI controllers; Operating conditions; Linear analysis; Efficiency

1. Introduction

Compared to other types of fuel cells, polymer electrolyte membrane fuel cells (PEMFC) have many advantages that make them suitable for a large number of applications. Some of these advantages are high power density, compactness, lightweight, low-operating temperature, solid electrolyte, long cell and stack life, low corrosion and high efficiencies [1]. PEMFC are regarded as ideally suited for transportation applications. However, important difficulties remain unsolved and a lot of research is being done in order to make the technology ready to implementation and commercialisation [2].

Advantages of different operating conditions for PEMFC have been described in the literature [3]. However, a comparison of the system controllability at different operating points is not found. A PEMFC can deliver the same amount of net power at different operating conditions. In order to chose the appropriate operating point, control aspects have to be taken into account, as well as efficiency aspects. Some works address the control of PEMFC [4–6], but only the efficiency is considered to determine the operating conditions. The objective of this work is to compare the controllability of a PEMFC operated at different operating conditions. The performance of the control system is evaluated implementing a diagonal structure with PI controllers in the control loops.

2. The model

In their study of the PEMFC flow dynamics, Pukrushpan et al. presented a control oriented model for an automotive application which has been the base for the model used in this work [4,7]. The transient phenomena captured in the model include the flow and inertia dynamics of the compressor, the manifold filling dynamics (both anode and cathode), reactant partial pressures and membrane humidity. On the other hand, the model neglects the extremely fast electrochemical and electrical dynamics, and temperature is treated as a constant parameter because its slow behaviour (time constant of 10^2 s) allows it to be regulated by its own controller. A constant cell temperature of 80 °C is assumed.

* Corresponding author. Tel.: +34 93 4015789; fax: +34 93 4015750.
E-mail address: maserra@iri.upc.edu (M. Serra).

0378-7753/$ – see front matter © 2005 Elsevier B.V. All rights reserved.
doi:10.1016/j.jpowsour.2005.10.092

Nomenclature

I_{st}	stack current (A)
K_c	proportional constant of the PI controller
p_{ca}	cathode pressure (bar)
P_{net}	net power (W)
T_i	time constant of the PI controller (s)
v_{st}	stack voltage (V)
v_{cm}	compressor voltage (V)
$W_{an,in}$	anode inlet mass flow rate (kg s^{-1})

Greek letters

Δ_p	anode–cathode pressure difference (bar)
λ_{O_2}	oxygen stoichiometry

Mass and energy balance are the basic laws for the different volumes being modelled. Constant properties are assumed in all volumes. Flowrates from one volume to another are calculated as a function of the upstream and downstream pressures. Ideal gases are assumed.

Membrane hydration captures the effect of water transport across the membrane. Water transport is modelled through drag and diffusion effects. Both water content and mass flow are assumed to be uniform over the surface area of the membrane. This surface is of 280 cm^2.

Stack voltage is calculated as a function of stack current, cathode pressure, reactant partial pressures, fuel cell temperature, and membrane water content. Identical behaviour of each cell is assumed and the stack voltage is calculated as the individual cell voltage per the number of cells, in this case 381.

The air entering the cathode is impelled by a compressor the model of which consists of a dynamic part and a static part read from an experimental compressor map. The modelled compressor has the angular velocity limited to 100 krpm, the exit flow limited to 0.1 kg s^{-1}, and the pressure ratio limited to 4. The power consumed by the compressor is the only parasitic power taken into account. The net power, P_{net}, is therefore calculated as the electric power given by the fuel cell minus the power consumed by the compressor. Cooler and humidifier are also included. It is assumed that a static humidifier supplies the air with the desired relative humidity before entering the stack.

At the anode side, entering hydrogen comes from a pressurised tank and the hydrogen flow is assumed to be a manipulated input variable.

Only one modification is introduced, which is the existence of an anode exit flow. This exit is necessary to control the hydrogen pressure along the flow channels and to improve the power demand transient responses [2].

Some of the indexes used for the linear analysis depend on the model scaling. One of the controlled outputs is the difference of pressure between anode and cathode, Δ_p. It has been scaled with a variation of 0.1 bar. To scale the rest of the input and output variables, a maximum variation of 10% has been assumed. Hence, the scaled variables are the non-scaled increments divided by the maximum increments.

SIMULINK linearisation tools have been used to obtain the state space matrices of the system at the studied operating points.

3. Operating conditions

This work is based on the analysis of a set of selected operating points. Their operating conditions are summarised in Table 1. In Fig. 1, the operating points are located on the curves of net power versus stoichiometry at different current values. In a fuel cell, a certain amount of net power can be obtained at different currents. OP1 to OP5 deliver the same net power, P_{net} = 37,400 W, and the same happens with OP6 to OP8, with P_{net} = 30,000 W. OP1 and OP7 have the minimum amount of current for which P_{net} of 37,400 and 30,000 W can be, respectively, obtained. For example, it is not possible to obtain 37,400 W of net power with a current lower than 175 A, at any pressure or stoichiometry. These operating points are specially interesting because minimum current corresponds to the minimum hydrogen consumption if the hydrogen that does not react is recycled. Looking at the different curves of Fig. 1, it can be seen that for small λ_{O_2} P_{net} increases when λ_{O_2} increases, but this trend changes from a certain λ_{O_2} value. This is because when λ_{O_2} is high, to increase λ_{O_2} requires a compressor power increase larger than the electric power increase obtained from the fuel

Table 1
Studied operating points

	P_{net} (W)	I_{st} (A)	λ_{O_2}	v_{st} (V)	p_{ca} (bar)	Efficiency (%)	v_{cm} (V)
OP1	37390	175	2.15	242.7	1.99	42.5	158
OP2		187	1.60	217.8	1.78	40.7	135
OP3			3.20	261.2	2.56	37.4	217
OP4		200	1.41	201.8	1.73	38.3	130
OP5		280	1.29	149.7	1.89	27.3	151
OP6	30000	134	2.37	254.2	1.86	44.9	142
OP7		150	1.25	209.5	1.49	41.4	100
OP8			3.89	273.94	2.55	36.6	214.0

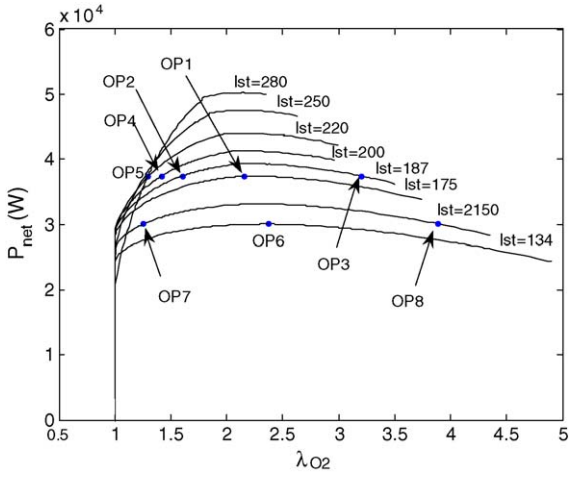

Fig. 1. Different operating points.

cell. Because of this power maximum, operating points with the same net power and current are possible (i.e. OP2 and OP3, or OP7 and OP8). It is interesting to compare these pairs of operating conditions that have different stoichiometries but the same net power and the same hydrogen consumption.

4. Control objectives

In this work, the stack current is considered a disturbance and there is a desired stack voltage, which depends on the required power. Therefore, the first control objective is to maintain v_{st} to the setpoint value. On the other hand, in order to prevent membrane damage, the difference in pressure between anode and cathode Δ_p needs to be small [8]. A small Δ_p will favour the membrane life time, and thus, the second control objective is to maintain Δ_p close to zero.

For certain applications, the required power is constant and there is a unique voltage setpoint. The selection of this setpoint (selection of operating conditions) is the main issue concerning this work. However, if the range of required power is large, different setpoint voltages will be necessary (even a desired operating curve), and what are the appropriate operating conditions will be questioned at every power level.

5. Structure of the control system

In this work, a decentralised PI based controller is implemented. Two output variables are controlled using two of the input manipulated variables giving a 2×2 control problem. The input control variable chosen to control v_{st} is v_{cm}. This control loop is called the first loop. To control Δ_p, $W_{an,in}$ has been chosen. This is called the second loop. From all possible pairs of manipulated variables, v_{cm} and $W_{an,in}$ have been chosen because this is what is found in the literature [4–6] and what is recommended after a controllability analysis by Serra et al. [9].

6. Tuning of PI controllers

The performance of the controlled system depends on the proportional and time constants of the PI controllers, K_c and T_i. In order to compare the behaviour of the proposed control structure at different operating points, it is important to employ the same tuning methodology. In this section, the used tuning methodology is described.

For the first loop, the control of v_{st}, Ziegler–Nichols tuning rules can be applied [10]. However, they are not appropriate for the second loop, the control of Δ_p, because the resulting tuning parameters provoke sudden changes in pressure that could damage the membrane. The tuning method used for the second loop permits to limit the pressure peaks. The tuning procedure consists of the following steps:

(a) *Tuning of the first control loop*. This tuning has been done with some tuning rules that can be viewed as a modification of the Ziegler–Nichols step response method: the Kappa–Tau tuning procedure [11]. These rules use three parameters to characterise the process dynamics instead of two, permitting substantial improvements in control performance while retaining much of the simplicity of the Ziegler–Nichols method.
(b) *Tuning of the second control loop*. The transfer function that relates Δ_p with $W_{an,in}$ is of second order, but has a zero and a pole which almost cancel each other. Eliminating the zero and pole, an equivalent first order transfer function is obtained. The methodology employed was proposed by Rivera et al. for disturbance rejection of low-order processes [12]. The proportional constant of the PI controller is calculated as a function of the steady state gain of the process, the time constant of the process, and a parameter that has been chosen such that Δ_p peaks are no larger than 0.3 bar when current steps of $40\,A\,s^{-1}$ and giving power increments of $\pm 20\%$ are applied.

Applying this tuning methodology to OP1, OP2, OP4 and OP5, the tuning parameters indicated in Table 2 are obtained.

7. Linear analysis

MIMO linear systems can be analysed using different analysis tools. These tools are mathematic operators applied to the transfer functions of the linear system. Some of them are applied to the process (without control) and characterise the controllability of the system as a property of the process itself. Others are applied to the controlled system and depend on the control structure and tuning. In this work, the following indexes and matrixes are considered in order to study the performance and controllability of the system: the Morari resiliency index (MRI), the condition number (CN), the relative gain array (**RGA**), the sensitivity function, **S**, and the complementary sensitivity function, **T**.

The MRI is the smallest singular value of the open-loop transfer function. It is the poorer gain of the process, poorer sensitivity, which corresponds to specific input and output directions. Large MRI over the frequency range of interest is preferred. The CN is the ratio of the maximum singular value to the minimum singular value. It indicates the sensitivity balance in a

Table 2
Scaled PI tuning parameters

	OP1		OP2		OP4		OP5	
	1st loop	2nd loop	1st loop	2nd loop	1st loop	2nd loop	1st loop	2nd loop
K_c	10.28	1.72	6.41	0.87	4.81	0.94	1.91	1.80
T_i	0.22	3.32	0.22	3.84	0.22	3.89	0.22	3.46

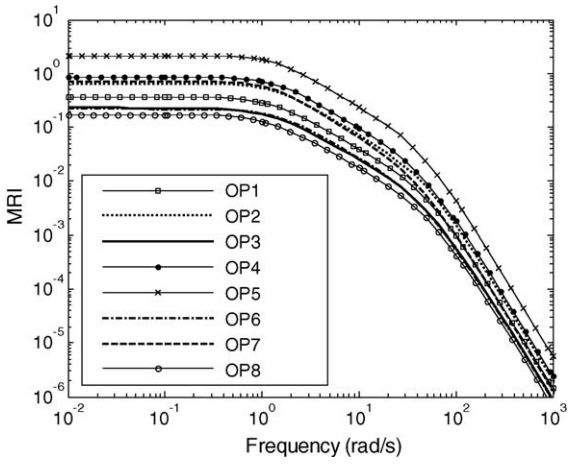

Fig. 2. MRI at the different operating points.

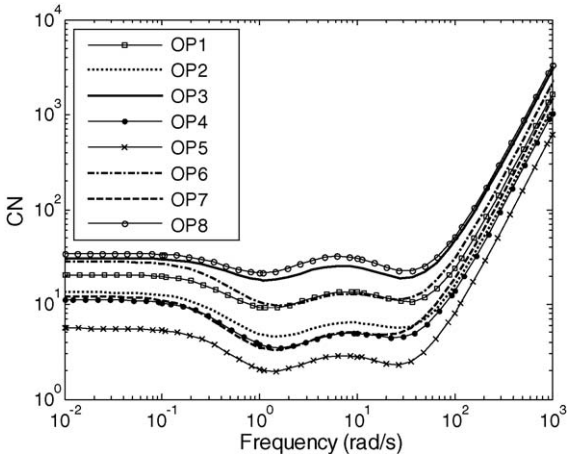

Fig. 3. CN at the different operating points.

multivariable system. Large CN indicate unbalanced sensitivity and also sensitivity to changes in process parameters. Therefore, small CNs are preferred. The **RGA** matrix is used to determine the interaction among control loops in a multivariable process. It is defined as the ratio of the open-loop gain for a selected output when all the other loops of the process are open, to its open-loop gain when all the other loops are closed. Pairings that have **RGA** close to unity matrix at frequencies around bandwidth are preferred. This rule favours minimal interaction between loops and prevents stability problems caused by interaction. Contrarily, large **RGA** elements indicate sensitivity to input uncertainty. **S** is a good indicator of the closed loop performance [13]. Typical specifications in terms of **S** include a large bandwidth frequency (frequency where the maximum singular value of **S** crosses 0.707) and a small peak of its maximum singular value. Large peaks indicate poor performance as well as poor robustness. Finally, **T** can be used to analyse the stability of the MIMO system [14]. The criterion require that the maximum value of its maximum singular value is small for robust stability. This maximum peak criterion can be insufficient for MIMO systems for which advanced tools considering uncertainty descriptions (μ-analysis) are needed. However, to have an idea of the stability robustness, this analysis can be useful.

The frequency range of interest is given by the bandwidth frequency, normally defined as the frequency up to which control is effective [13]. The range of frequencies analysed in this work is $0–10^3$ rad s^{-1} because it is assumed that the bandwidth will be within this range. In Figs. 2–4, the MRI, CN and RGA(1,1)

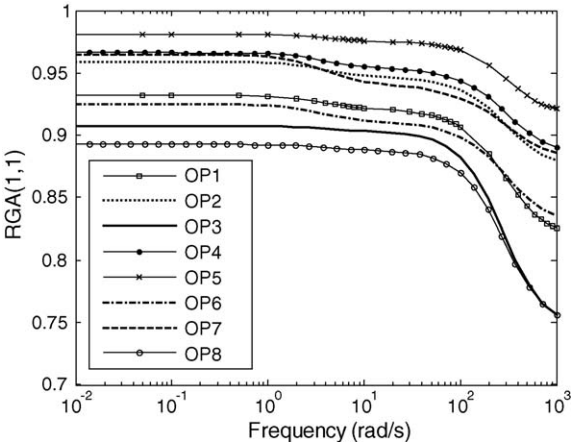

Fig. 4. **RGA** at the different operating points.

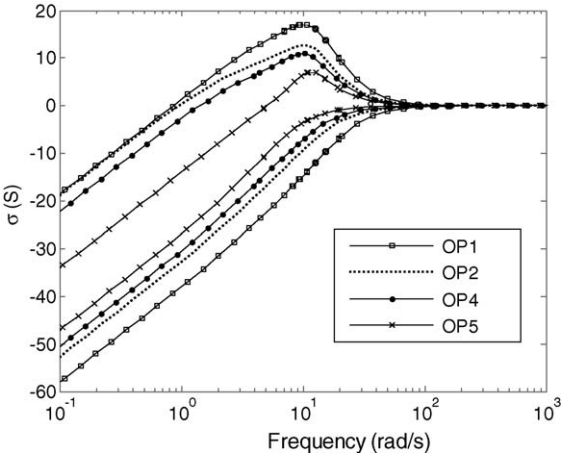

Fig. 5. Maximum and minimum **S** singular values.

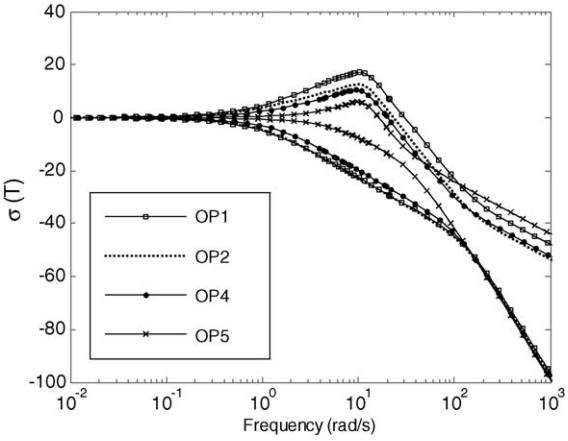

Fig. 6. Maximum and minimum **T** singular values.

of the 2X2 system are plotted. The three controllability indexes indicate the same trends: comparing OP1, OP2, OP4 and OP5, the controllability improves when the current increases. OP5 has the highest MRI, the lowest CN and the **RGA** closest to 1, followed by OP4, OP2 and OP1. Comparing these operating points with OP3, results indicate the poorest controllability at OP3. It can be seen that differences remain important all long the analysed frequency range.

If the analysis is repeated at a different P_{net} level, 30,000W, similar results are found: OP7 has better controllability than OP6, and OP8 has the poorest controllability of the three.

The sensitivity function, **S**, and the complementary sensitivity function, **T**, are also calculated for the controlled system at OP1, OP2, OP4 and OP5, using the tuning parameters indicated in Table 2. The maximum and minimum singular values of these matrixes are shown in Figs. 5 and 6. The following conclusions can be deduced from the Figures: the controlled system is faster at OP5 (higher bandwidth), and the peaks are lower for OP5, indicating better performance and robust stability. Therefore, from a control point of view, OP5 is the best, followed by OP4, OP2 and OP1.

8. Simulation results

In order to take into account the influence of the non-linearities, different simulations are done with the non-linear model. Figs. 7–14 show the behaviour of the controlled system in front of current and voltage setpoint step changes. Simulations are done around OP1 and OP5. All the combinations of 0 and ±10% increments in I_{st} and v_{st} setpoint are applied, covering eight equidistant directions of the bidimensional space defined by these two inputs. The dashed lines correspond to the ±10% current increments without v_{st} setpoint changes. Figs. 7, 9, 11 and 13 correspond to operation around OP1, and Figs. 8, 10, 12 and 14 correspond to operation around OP5.

One first general result is that at OP5 the system responds in a more regular manner in all directions. This confirms a lower system directionality at OP5. For instance, in Fig. 7, oscilatory behaviour is seen in the lower curves, which correspond to negative steps in the v_{st} setpoint, and not in the upper curves, which correspond to positive steps in v_{st} setpoint. In Fig. 8, small peaks are seen in the lower curves, which correspond to negative steps

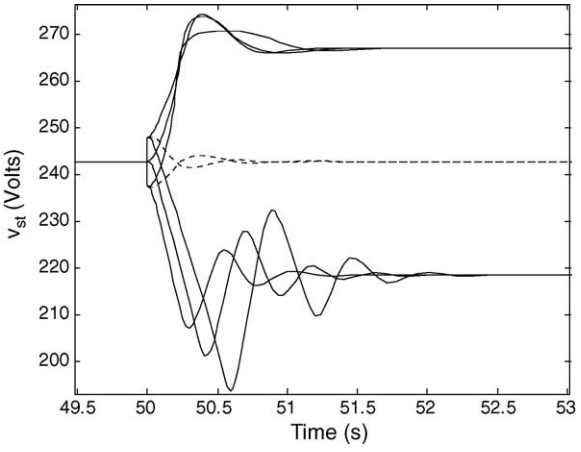

Fig. 7. v_{st} response at OP1.

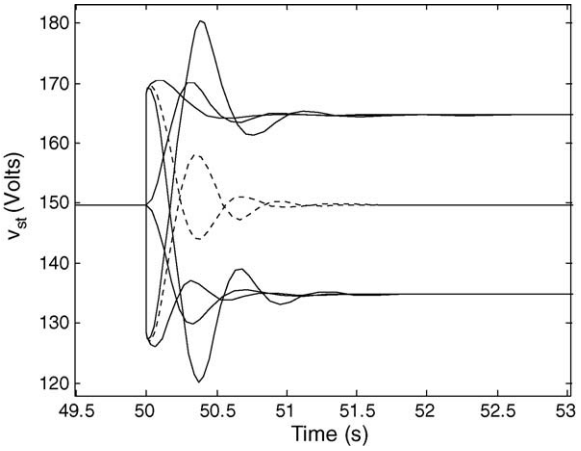

Fig. 8. v_{st} response at OP5.

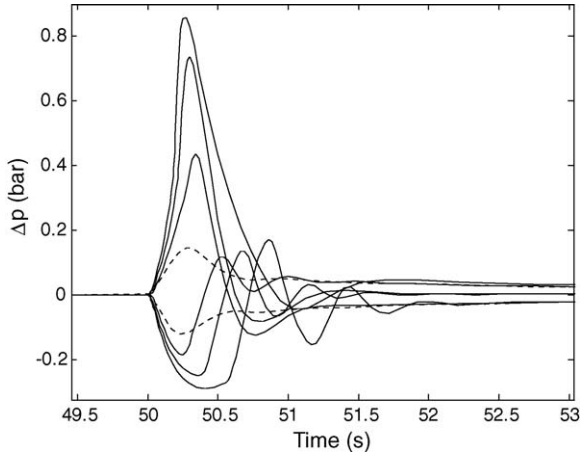

Fig. 9. Δ_p response at OP1.

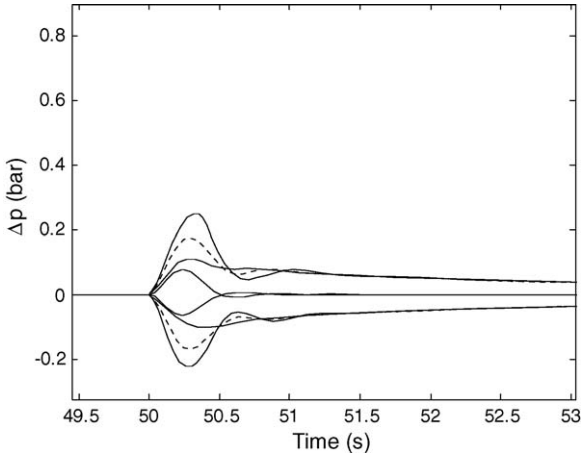

Fig. 10. Δ_p response at OP5.

in the v_{st} setpoint, and large peaks are seen in the upper curves, which correspond to positive steps in v_{st} setpoint. Comparing Figs. 7 and 8, while similar v_{st} peaks are found, a faster control is obtained at OP5. The worst oscillations are found at OP1. Looking at Δ_p, peaks are larger at OP1. In Figs. 11 and 12, it can be seen that v_{cm} has much larger increments and oscillations around OP1. Finally, in Figs. 13 and 14 a better behaviour is found around OP5 as well, with faster response, smaller peaks, and less oscillations.

To analyse the controlled system behaviour in front of larger disturbances around OP1 and OP5, current steps of −24 and +30% (corresponding to ±20% of net power) have been applied. Simulations show a similar behaviour of v_{st} and Δ_p at the two operating points, but both v_{cm} and $W_{an,in}$ have larger peaks at OP1.

Therefore, simulation results agree with the linear analysis that the analysed fuel cell system has better control properties at OP5. Moreover, for the analysed variables and within the scope of this work, it can be said that the performance of the proposed control system around OP5 is satisfactory.

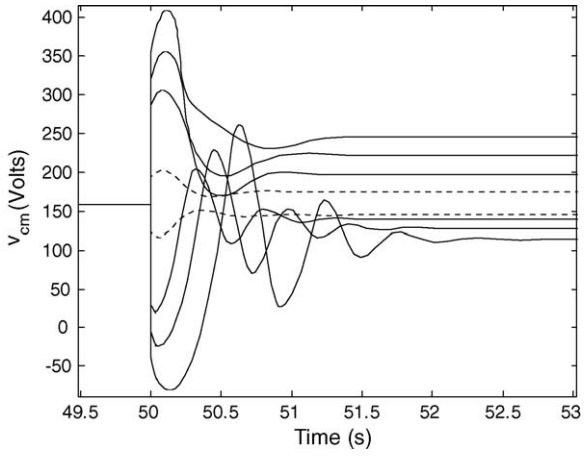

Fig. 11. v_{cm} response at OP1.

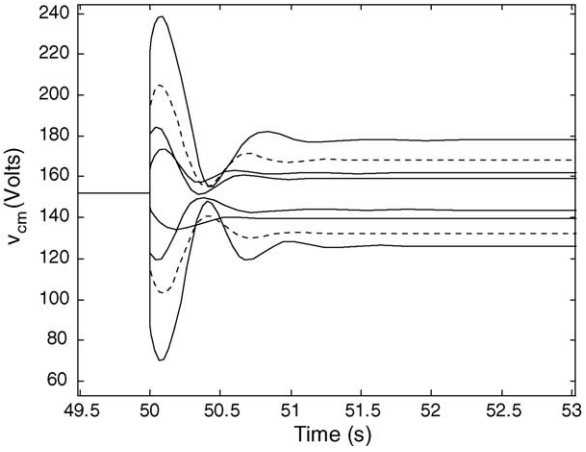

Fig. 12. v_{cm} response at OP5.

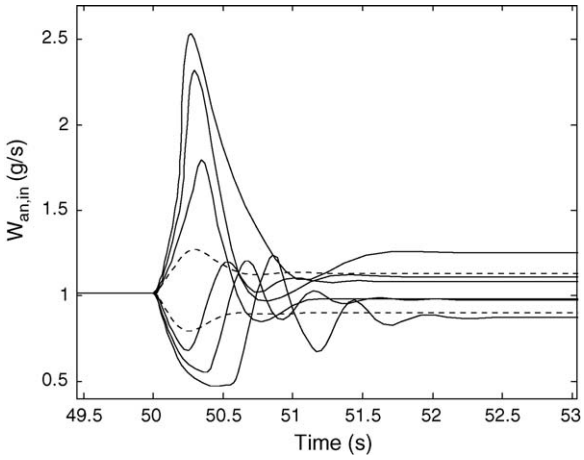

Fig. 13. $W_{an,in}$ response at OP1.

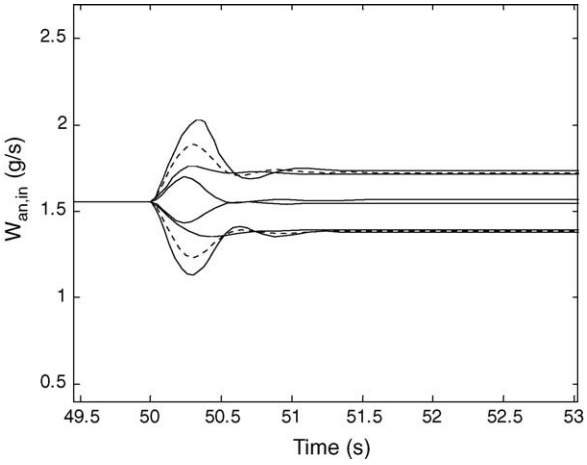

Fig. 14. $W_{an,in}$ response at OP5.

9. Conclusions

Using three different controllability indexes (the MRI, the CN, and the RGA) to compare the controllability of a PEMFC at different operating points, it has been found that the higher the efficiency, the lower the controllability. Having done the comparative analysis at different net power levels, it can be said that the conclusion is valid in a wide operating range. Comparing operating points with the same current and net power but different stoichiometry and output voltage, the operating points with higher stoichiometry (higher output voltage) have the worst controllability. To continue the comparison, using some performance tools (the sensitivity functions S and T) results also indicate that it is easier to control the system when it is operated at the operating point with lower efficiency. Finally, some simulations done with a complete non-linear model show the same trend. Therefore, comparing the controllability and performance of a controlled PEMFC at different operating conditions, it has been found that there is a trade-off between controllability and efficiency within a wide operating region. The compressor has a key influence on the controllability and the efficiency of the system.

A diagonal control structure with PI controllers in the control loops is implemented and a tuning procedure has been proposed. For the analysed variables and within the scope of this work, it can be said that the performance of the proposed control system around OP5 is satisfactory.

Acknowledgments

This work has been funded partially by the projects CICYT DPI2002-03279 and CICYT DPI2004-06871-C02-01, of the Spanish Government.

References

[1] L. Carrette, K.A. Friedrich, U. Stimming, Fuel cells—fundamentals and applications, Fuel Cells 1 (2001) 1.
[2] W. Yang, B. Bates, N. Fletcher, R. Pow, Control challenges and methodologies in fuel cell vehicle development, in: International Congress of Transportation Electronics 98C054, 1998.
[3] J. Larminie, A. Dicks, Fuel Cell Systems Explained, John Wiley & Sons Ltd., 2003.
[4] J. Pukrushpan, A.G. Stefanopoulou, H. Peng, Control of fuel cell breathing, IEEE Control Systems Magazine (April) (2004).
[5] M. Grujicic, K. Chittajallu, J. Pukrushpan, Control of the transient behaviour of polymer electrolyte membrane fuel cell systems, Proc. Inst. Mech. Eng. Part D: J. Automobile Eng. 218 (2004).
[6] A. Vahidi, A. Stefanopoulou, H. Peng, Model predictive control for prevention starvation in a hybrid fuel cell system, in: Proceedings of the American Control Conference, vol. 1, 2004, pp. 834–839.
[7] J.T. Pukrushpan, H. Peng, A.G. Stefanopoulou, Control-oriented modeling and analysis for automotive fuel cell systems, Trans. ASME 126 (March) (2004).
[8] S. Yerramalla, A. Davari, Dynamic modelling and analysis of polymer electrolyte fuel cell, IEEE (2002).
[9] M. Serra, J. Aguado, X. Ansede, J. Riera, Controllability analysis of decentralised linear controllers for polymeric fuel cells, J. Power Sources 151 (2005) 93–102.
[10] K. Ogata, Modern Control Engineering, Prentice Hall, 2002.
[11] K. Astrom, T. Hagglund, PID Controllers: Theory, Design and Tuning, ISA, 1995.
[12] D. Rivera, S. Skogestad, M. Morari, Internal model control 4: PID controller design, Ind. Eng. Chem. Process Des. Dev. 25 (1986) 252–265.
[13] S. Skogestad, I. Postlethwaite, Multivariable Feedback Control, Analysis and Design, John Wiley & Sons, 1996.
[14] W. Luyben. Process Modeling, Simulation and Control for Chemical Engineers, 1990.